AN ATTEMPT TO OBSERVE THE EARTH LIQUID CORE RESONANCE WITH EXTENSOMETERS AT PROTVINO OBSERVATORY

E.A. Boyarsky[1)], B. Ducarme[2)3)], L.A. Latynina[1)], L. Vandercoilden[3)]

[1)]*Gamburtzev Institute for Physics of the Earth, RAS, Moscow*

[2)]Chercheur Qualifié FNRS, [3)]*Royal Observatory of Belgium, Brussels*

ABSTRACT

We performed a tidal analysis of the strain records obtained at the Protvino observatory near Moscow during the years 1995–2000. The deformations were measured with four 16 m long extensometers installed in the NS and EW directions at a depth of 15 m. This study is focusing on the liquid core resonance effect. We are using the ratios of the amplitude factors of the resonant waves K1 and P1, to the amplitude factor of the static wave O1. The ratios are in principle free from indirect effects, such as cavity effects, which are roughly similar for all the diurnal waves. The resonance effect is clearly recognized in the measured ratios, especially in EW direction. The main cause of discrepancy between the observed and theoretical values of the resonance is the diurnal outer temperature variation, while the influence of the inner temperature and of the atmospheric pressure is many times lower. The temperature response was first directly evaluated as additional unknown in the tidal analysis and was also computed for various time shifts τ of the temperature signal. As the improvement was not so effective for the NS component a special study was performed. An attempt was made to determine the temperature response from the S1 wave alone or to include also the time derivative of the temperature. All attempts gave similar results: the temperature compensation increases the amplitude of K1 and decreases the amplitude of P1, while O_1 is practically not affected. K1 becomes closer to the expected resonant value. It is not quite clear, to what extend the correction, simply based on the outer temperature variations, is physically valid, as the perturbations are due to the thermoelastic strains. In their turn, the latter can be governed by the spatial distribution of the surface temperature and the mechanical properties of the rocks, including not only their values but also their spatial and temporal gradients.

1. Introduction

The tidal deformations depend on the regional and local features of the Earth crust and mantle. Tidal deformation monitoring is useful for the studies of the structure and evolution of crustal blocks, in zones of active tectonic processes of natural and industrial origin [Starkov et al. 1992]. Data collected by the tidal gravity networks are contributing to the determination of the regional irregularities of the Earth crust and upper mantle [Yanshin et al. 1986].

Extensometer data can be used in global problems such as the investigation of the nearly diurnal resonance of the Earth liquid core. This resonance, on a frequency 1.004915 cycle per solar day, disturbs the amplitudes of tidal diurnal waves with close frequencies i.e. P_1 and K_1. The tides and the forced nutations are produced by common gravitational forces but expressed in alternative coordinate systems: the nutations—in the inertial one, the tidal oscillations —in the terrestrial one. The corresponding frequencies differ only by the sidereal frequency 1.0027379 cycle per solar day. The Tidal wave K_1 corresponds to the precession, while the tidal wave P_1 corresponds to the half-yearly nutation. The forced nutations are globally observed using the techniques of astronomy and space geodesy. The tides are studied locally by geophysical methods. Until recently the earth tidal observations played a prevailing role in investigation of the Earth core resonance effects. In the last decades the vigorous progress of the space geodesy inversed the roles. Nevertheless, precise tidal gravity observations by means of superconducting gravimeters open new perspectives in the investigation of the liquid core resonance effects as they register reliably the tidal waves P_1, K_1, PHI_1 and PSI_1 which are the closest to resonance and hence highly influenced (Ducarme & al., 2002). The extensometers have an essentially lower precision. But they hold much promise if one considers that changes of the Love numbers at frequencies near to resonance induce relative disturbances in strain that are ten times larger than in gravity tide (Fig.1).

The theory of the luni-solar nutations and tides, taking into account nearly diurnal resonance of the liquid core, was developed by M.S.Molodensky [1961] and became the basis for numerous works later.

The most thorough computations of the body tide for rotating earth, having elliptic stratification, self-gravitation and a solid inner core, were performed by J.Wahr [1981] for different models of the Earth. New approaches to the data analysis for the forced and free nutations of the Earth allowed to E.Groten and S.M.Molodensky [1996] and S.M.Molodensky [1999] to create an optimal model of the tides. Using modern VLBI-observations, they determined with a significant accuracy the Q-factors of the bottom mantle and the dynamical flattening of the liquid core. Dehant & al. [1999] proposed tidal models including non hydrostatic flattening of the Earth and inelasticity in the mantle. Mathews & al. [2002] introduced a magnetic coupling between core and mantle.

Let us consider the theoretical amplitude of the diurnal tidal deformations in two orthogonal directions [Melchior 1972]:

for NS: $A_{\theta\theta} = W_2 / ag \times (h - 4l) = A \times (h-4l)$,

for EW: $A_{\lambda\lambda} = W_2 / ag \times (h - 2l) = A \times (h-2l)$.

Here W_2 is the tidal potential of degree two, a is the equatorial radius of the Earth, g is gravity at its surface, h and l are the Love's and Shida's numbers for a given tidal frequency. An effect of the liquid core resonance appears as changes in the numbers h and l and can be determined from the amplitude factor $\varphi_{xx} = A_{xx}/A$ of a resonant tidal wave. The amplitude factor of a single wave is not adequate for determination of resonance effect as far as an observed amplitude contains always "indirect" effects associated with topography, irregularities of geology etc. But these indirect effect are almost the same for all the diurnal tidal waves and can be eliminated by considering the ratio of the amplitude factor of a resonance-disturbed wave to that of an undisturbed wave [Latynina 1983].

We shall thus estimate how the resonance affects the waves P_1 and K_1 by taking ratios of their amplitude factors φ_{xx} to that of O_1. The amplitudes of these three waves are rather large and measured reasonably well. The wave O1, which is far from resonance, is chosen as reference. The resonance changes the amplitude of a wave close to it, so the ratio of its amplitude factor to that of O_1 becomes different from one. Theoretically estimated ratios vary in a small range of 1 to 2 percent according to the different Earth models. The averages for NS and EW components for different models are:

$\varepsilon_{P1} = \varphi_{NS}(P_1) / \varphi_{NS}(O_1) = 0.90$ $\varepsilon_{K1} = \varphi_{NS}(K_1) / \varphi_{NS}(O_1) = 0.65$ $\eta_{P1} = \varphi_{EW}(P_1) / \varphi_{EW}(O_1) = 0.94$ $\eta_{K1} = \varphi_{EW}(K_1) / \varphi_{EW}(O_1) = 0.80$.

In opposition to Polzer at al. [1996] we consider here the ratio of the amplitude factors but not their difference.

2. Data analysis

We are studying here the extensometer measurements made at Protvino observatory (54º52´ N, 37º13´ E) located 100 km southward from Moscow. The quartz 16-m extensometers are placed at a depth of 15 m in horizontal galleries along NS and EW directions (Fig.2) [Latynina et al. 1997, Boyarsky et al. 2001]. The enclosing rocks consist of sandstone and marl layers and jointed limestone. During the years seventies and eighties analog recording was used, and time registration was not accurate. As a result, only some short observation series could be taken for the tidal analysis [Karmaleeva 1999]. In this work we use only the observations of 1995–2000. However the most reliable data are available since digital acquisition systems were installed, with 12-bit ADC in 1998 and 16-bit ADC in 1999.

The harmonic analysis of the measurements is performed with Eterna 3.0 program [Wenzel 1996], using the Pertsev filter with a length of 51 hours. The measurement intervals in Table 1 overlap slightly. Otherwise they would be too short for the separation of the waves P_1, S_1, and K_1, which requires one year time interval. Detailed analysis results (Tables 2 to 5) are given only for the most reliable part (1999–2000). The results of the three EW strainmeter signals are rather coherent. The discrepancy is of

the order of 5% on the main wave O_1 (Table 6).

For the NS component the value of ε_{K1}, reflecting FCN resonance effects, significantly differs from the theoretical model (Table 1). The difference is still large if one takes only the more reliable recent measurements. The average EW ratio η_{K1} from three intervals is not so far from the rated one. But for the wave P_1, which has less resonance effect, the observed ratio η_{P1} contradicts physical notions. For the years 1999–2000 the discrepancies between observed and theoretical values of η are larger than 10%. However the comparison of the three EW extensometric signals for the same time interval 1999–2000 (Table 1) confirms that the η values are in good internal agreement: 2% for P_1 and 6% on K_1. The use of the amplitude ratios did not suppress the systematic errors. According to hydrological measurements in the borehole, diurnal level variations of the upper aquifer at a depth of 25 m are less than 1 cm. There are no more accurate and complete related data, so this point needs further studies. To our opinion, the remaining discrepancy with the theoretical value is mainly associated with the meteorological noise.

3. Influence of temperature variations on tidal amplitudes

The measurements are affected by meteorological influences. That can be seen directly from the extremely large values of wave S_1 in Tables 2 to 5. Its amplitude factor in the reliable data of 1999–2000 was 67.3 for NS direction and 30.2–32.9 for the strainmeters in EW direction. The simplest way to compensate meteorological influences is to evaluate the responses (regression coefficients) R to selected meteorological parameters. We have thus to find the perturbation mechanism. The direct exposure of the deformation sensors to temperature variations is small. The seasonal temperature wave inside the galleries reaches only 0.3°, and the diurnal variations do not exceed 0.01°, as long as nobody is entering the station. Induced errors on the capacity sensors are an order of magnitude lower than the observed diurnal deformations, and thermo-expansion of the extensometer quartz tube is tens times less than that of enclosing rock. It is of much importance, that the spectrum of temperature inside the stations contains only noise near the frequency 1 cycle per day (Fig. 3, below). On the contrary, the spectrum of the outer temperature (Fig.4) contains, as it should be, a sharp peak at the frequency one cycle per day with side lobes at the P_1 and K_1 frequencies which represent the annual modulation of S_1. The whole resonance spectrum will thus be disturbed. It appears, that the most probable sources of transfer of the heat disturbances are thermoelastic deformations of rocks, induced by the outer temperature variations, that propagate tens of meters down.

Consequently, we introduced in the harmonic analysis of the 1999–2000 data sets linear regression coefficients of the observed deformations with respect to the air temperature registered at Serpukhov weather station, 15 km apart as well as to the atmospheric pressure at Protvino observatory (Table 7). The discrepancies between the model values of ε and η and the observed values are largely reduced for K1, especially in EW direction, but P1 is not improved. The atmospheric pressure influence is one order of magnitude lower than the temperature effect. An account of the response to the pressure decreases A_{S1} and residuals but only by few percents (Table 7). A time shift of pressure values in any direction does not affect results.

Therefore the main attention was paid to the temperature effects. The temperature influence was studied at various time shifts τ of the temperature relative to observed deformations, namely $-50^h < \tau < 50^h$ (Fig. 5–6). With this convention a positive time shift of the perturbing signal corresponds to a "time lag" of the strainmeter response. The graphs for the two other EW extensometers are omitted, because they are practically identical to Fig.6. It is supported once more, that the wave O1 is free from diurnal temperature variations. Criteria for the best compensation of temperature effect can be: minimum amplitude A_{S1} of the wave S1, minimum standard deviation s_0 of residuals, maximum absolute value of response R. It is pertinent to note that a behavior of $R(\tau)$ is equivalent to a cross-covariance function.

Diurnal oscillations of R and double-frequency oscillations of A_{S1} and s_0 are explained with repetitive temperatures on adjacent days. These oscillations, naturally, decay with moving from $\tau = 0$ in both direction. In general, a time lag of thermoelastic deformations with respect to temperature variations is quite possible, especially at a depth of 15 m, but not with a lag of 12 or 24 hours, which are only mathematical artefacts. Regional thermoelastic deformations of hundreds kilometers in dimension can be associated only with very small τ of less than one hour. A similar influence of atmospheric pressure variations for tiltmeter measurements has been already reported [Boyarsky et al. 2001]. But any negative τ can meet objections because it is hard to model a physical mechanism that manifests itself in deformations preceding the temperature variations, except if we consider that the effect depends also of the gradients of the harmonic exciting functions.

For the three EW instruments a minimum A_{S1} and the best coincidence of the observed resonance effect with the theoretical one for K1 occur at time shifts of –0.5, –0.4, and -0.6^h. However, minimum s_0 and maximum R occur uniformly at shifts of +2.3, +2.2, and $+2.1^h$, with values η_{K1} close to 0.75.

With temperature correction, the amplitude A_{S1} for NS component decreases 4–5 times. Minimum A_{S1} corresponds to a shift $\tau = -0.8^h$ (Table 9), and simultaneously the deviation of the ratio $\varepsilon_{K1} = 0.55$ from its theoretical value 0.65 is minimum (14%) almost at the same τ. Maximum R (0.956 nstr per degree) is at $\tau = +0.6^h$, and the same shift is just a minimum for s_0. Minimum ε_{P1} is rather near ($\tau = +0.9^h$), but corresponds to a maximum of discrepancy with the model. Another criterion to check if the temperature correction is optimal can be the wave K1 phase shift κ_{K1} (Table 9) that should become minimum. Its minimum 1.9 degrees is at $\tau = +2.0^h$.

As already pointed out, a positive time shift τ is preferable from a physical viewpoint as it corresponds to a time lag of the elastic response of the rock. Moreover the oscillations of both s_0 and R decay faster than A_{S1} with larger time shifts. Therefore, the criterion of minimum s_0 and maximum R is better, at least in our case, than the criterion of minimum A_{S1}. It is confirmed by an additional test. We introduced the temperature signal together with its time derivative to derive the optimum phase lag of the strain coupling. It is justified by the fact that the temperature signal is largely dominated by S1 and can be written in first approximation as

$$T = A \cos w_1 t \qquad (1)$$

and the strain response as

$$RA \cos(w_1 t - k) = R_C A \cos w_1 t + R_S A \sin w_1 t \qquad (2)$$

where R is the response and k the phase lag of the system.

Using the temperature and its time derivative we get

$$R^*_C A \cos w_1 t - w_1 R^*_S A \sin w_1 t \qquad (3)$$

and can derive easily (R_C, R_S) from (R^*_C, R^*_S) and thus R and k.

Experimentally we obtained (Table 9) $R = 0.973$, $k = 8°.5$, $t = 0.56^h$, $s_0 = 3.162$. We effectively confirm that a maximum of R and a minimum of s_0 corresponds to a lag of 0.6^h.

The influence of seasonal temperature variations on tilts at Protvino was studied by the authors [Boyarsky and Latynina 1999, Latynina and Boyarsky 2000]. The analysis of short tiltmeter observation series showed that the amplitude of the diurnal waves varies during a year more than twice. Temperature

variations affect the measurements with 16 m extensometers to much less extend, especially as they are averaged on rather long series. But the aim of this work—the study of resonance effects—requests very precise tidal parameters.

Temperature disturbance of the gravity tide were studied in details by T.Chojnicki [1987] for Askania GS–11 gravimeters. By means of iterations the temperature wave S1 was eliminated from the observations. The decrease of A_{S1} and s_0, computed from corrected observations, was taken as a criterion. However, the method does not give accurate quantity estimates. Besides, the final result can depend upon the initial choice of the parameters of the nearly diurnal tidal waves, which have been subtracted from the observed data at the very first stage.

The waves P_1, S_1, K_1 are heavily disturbed by temperature variations. It is easily explained by the characteristics of these variations. The amplitude of diurnal temperature wave S1 is changing along a year. For example, the diurnal variations of the outer temperature at Protvino in summer are about twice larger than in winter. It can be sketchy presented by modulating the amplitude of S_1 by a wave of one year period [see also Merriam 1994]:

$$T(t) = A\ \{1 + B\ (\cos \omega_2\, t)\}\ (\cos \omega_1 t), \qquad (4)$$

where ω_1 = 1/day, ω_2 = 1/365.25 day = 0.00273785. Hence:

$$T(t) = A \cos \omega_1 t + AB\{\cos(\omega_1 + \omega_2)\, t + \cos(\omega_1 - \omega_2)\, t\}. \qquad (5)$$

Thus, the yearly amplitude modulation of the diurnal temperature wave is equivalent to producing waves with frequencies $(\omega_1 - \omega_2) = 0.99726$ and $(\omega_1 + \omega_2) = 1.00274$, but these are just the frequencies of P1 and K1.

This is clearly seen on the spectrum of the outer temperature (Fig.4), in which we can see not only a sharp diurnal peak with amplitude of 2.3 degrees but also waves with frequencies of 1.0027 and 0.9973 and an amplitude reaching 1.6 degree. Detectable harmonics with frequencies $(\omega_1 + n\omega_2)$, where $n = \pm 2$, ± 3 etc, indicate a more complicated temperature trend than the simplest model above. Note that at $n = +2$ and $n = +3$ we deal with tidal waves PSI_1 and PHI_1 which are the closest to the resonance.

A direct compensation of the temperature influences with Eterna program (Table 7), even with the application of various time shifts (Fig. 5–6 Table 9), decreased the discrepancy between observed and rated resonance effects for K_1 but not for P_1, especially in NS component. This problem led us to compute directly the contribution of thermoelastic deformations to amplitudes of P_1 and K_1. As well as in Eterna program, it was assumed, that the thermoelastic part of each diurnal wave is proportional to the corresponding temperature variation, namely

$$D(t) = RT(t + \tau), \qquad (6)$$

where D is the temperature contribution to the observed deformation. The outer temperature was treated by Eterna program with the identical parameters and on the same time intervals as NS deformations of 1999–2000 (see Table 8, row 3). We assume the adjacent waves have similar response R and phase shift κ. The observed deformation wave S1 is almost entirely of weather origin, mostly of temperature. It makes possible to find the common characteristics R and κ from S1 and calculate thermoelastic contributions to waves P_1 and K_1 which should be subtracted from measured deformations. We find for the thermal S1wave a phase shift of –7.2° with respect to the strain wave, corresponding to a time shift of 0.48^h. Here also P_1 amplitude decreases after correction while K_1 increases. It should be noted that the phase difference becomes closer to zero (Fig.7) in better agreement with the theoretical tidal waves.

The calculated response of –0.75 nstr/Kelvin is rather similar to the value obtained by Eterna program for the global tidal signal. A negative value of R means that rocks compress at depth when outer temperature increases. An incomplete compensation of weather noise in K_1 and no compensation in P_1 imply, that temperature effects are not correctly taken into account or that some weather factors are

ignored. Perhaps, the analysis should be made separately for all the summer and all the winter observations, but we have not yet enough reliable data for that.

The discrepancy between observed and theoretical resonance effects can be associated with a non-adequate model of development of thermoelastic strains. Eterna program assumes linear regression between the rock deformation and the temperature variations. Nevertheless, thermoelastic deformation can be due as well to surface temperature gradients or irregularities of earth crust surface layers, including topography. Let us write the temperature variations be a function of time and place in a form:

$$T(t,x) = A \sin(\omega_1 t)\,(1 - p \cos(x/L)), \qquad (7)$$

where p is a constant, and L is length of temperature wave on earth surface along X axis. Then the temperature gradient along X axis is

$$\text{grad}(T) = (A\,p/L) \sin(x/L) \sin(\omega_1 t). \qquad (8)$$

If the wavelength L does not vary with time, then the responses of the crust to the temperature and its gradient differ only in a constant factor $C = L \sin(x/L)$. Therefore, the attempted compensation of temperature noise is still valid.

Suppose the wavelength L varies with time. This is rather possible because in winter the snow levels off the contrasts in spatial distribution of surface temperature due to the various albedo's of forest, field or water. In this case L can be represented, for example, as

$$L = 1 / (a_1 + a_2 \cos \omega_2 t), \qquad (9)$$

where ω_2 is frequency of the yearly wave, a_1 and a_2 are constants. As a result, the harmonics with frequencies $(\omega_1 - 2\omega_2)$, wave PI_1, and $(\omega_1 + 2\omega_2)$, wave PSI_1, will appear in the temperature spectrum. But we could not detect reliably those harmonics in the strain signal, even if we combine all the data at our disposal.

The surface temperature distribution and the structure of the very upper crust layers have a complicated character. It is possible to create a model of thermoelastic deformations corresponding to the conditions of Protvino observatory. Temperature gradients can be associated with the regional geologic structures. Rather monolith blocks of some kilometers in dimension are separated by ancient fracture zones. Under such situation the wavelength L should be comparable with the block dimensions. A differential warming up of ground under the observatory building and its immediate grass surrounding can be a cause of intensive thermoelastic deformations as well. The extensometers themselves are placed in such a manner, that one end of each is under the observatory building, and the other is 10 m apart from the building. Temperature wavelength can have an order of some tens meters. It is very hard to eliminate errors induced with local irregularities. Nevertheless, these considerations should be kept in mind when choosing a place for future observations.

4. Conclusions

The tidal strain deformations at the Protvino observatory, near Moscow, are studied for the period 1995–2000. The deformations were measured with four 16 m extensometers at depth of 15 m (one along NS direction, and three along EW). The computations were made with Eterna 3.0 on three time intervals, more than 1 year each. The total data set exceeds 1200 days. Differences in amplitudes of the main waves from the three parallel EW extensometers do not exceed 3%, increasing our confidence in the analysis results.

We studied the liquid core resonance effect through the waves K_1 and P_1, using the ratios of their amplitude factors to the amplitude factor of wave O_1. We proceeded from the assumption, that the ratios are free from indirect effects as they are roughly similar for all the diurnal waves. The wave O_1 was taken as reference because its amplitude is of the same order and almost free from resonance effect. The

observed resonance disturbances is close to the rated values in the EW direction but not for NS direction.

The main cause of discrepancy between observed and theoretical values is diurnal outer temperature variations. They are responsible of more than 90% of the anomalous large amplitude of the wave S_1. The atmospheric pressure influence is many times less. The data of an adjacent weather station were taken for the compensation of temperature effects. The temperature was taken as auxiliary parameter in the tidal analysis using Eterna 3.0 software. The compensation was also studied at various time shifts τ of the temperature relating to the observed deformation. The shift τ for minimum amplitude of S_1 does not coincide with the shift that gives maximum response R and minimum standard residual s_0.

For EW component observed resonance effects for both P_1 and K_1 become close to the theoretical ones. For NS component a summary of the results is given in Table 9. All attempted corrections give similar results: ε_{P1} decreases while ε_{K1} increases and becomes closer to the reference model. The amplitude of S_1 is minimum at $\tau = -0.8^h$. At -1^h shift there is a minimum discrepancy between observed (0.55) and theoretical (0.65) resonance effects for ε_{K1}. For P_1 the temperature compensation gave almost no result. However from a physical point of view we should assume that the ground response follows the temperature excitation and thus that the time shift of temperature has to be positive. It is confirmed by the fit of the temperature and its time derivative which gave the best fit (s_0=3.162) and a response of -0.973 nstr/K for a time shift of 0.56h. Unhappily e_{K1}=0.506 is still far from the model (e_{K1}=0.65).

For comparison the tidal waves amplitudes were estimated by computing direct corrections from the temperature waves for P_1 and K_1, under assumption that the S_1 wave is purely of meteorological origin. The amplitude and phases of these temperature waves were computed from a three-years series of outer temperature.

All methods gave similar results: rocks compress at a depth when outer temperature increase and the coefficient is close to –0.9 nstr/Kelvin. Temperature compensation increases amplitude of K_1 and decreases amplitude of P_1. K_1 becomes closer to the theoretical resonance.

There are many possible causes for the incomplete compensation of weather influences. Hydrological effects are not yet investigated in details. It is not quite apparent, to what extent the compensation of outer temperature variations is valid at all. Errors in observations are associated with thermoelastic strains that, in their turn, can be governed with spatial distribution of surface temperature and mechanical features of rocks, taking into account their gradients as well. The applied procedure is valid, if the spatial distribution of temperature does not vary with time. In this case the responses of deformation to the temperature and its gradient differ only in a constant factor. When temperature variations have a seasonal pattern, the temperature spectrum is perturbed by harmonics with frequencies near the tidal waves PI_1 and PSI_1. The spectrum of the thermoelastic deformations becomes different from the temperature spectrum. Investigation at the PSI_1 and PHI_1 frequencies require more data than at our disposal.

References

1. *Boyarsky, E.A. and Latynina, L.A.*, 1998. The analysis of the tidal parameters on short measurement intervals. Bull. Inf. Marées Terrestres, **130**, 10050–10057.
2. *Boyarsky E.A., Vasil'ev I.M., and Suvorova I.I.*, 2001. The study of tilts and strains at the Protvino geophysical station. Izvestiya, Physics of the Solid Earth, **37**, No 9, 764–770.
3. *Chojnicki, T.,* 1987.Temperature distortion of tidal observations // Publications of the Institute of geophysics, Polish Academy of Sciences, F–14 (200). Warszawa–Lodz, 1987, 127–141.
4. *Dehant, V., Defraigne, P. and Wahr, J.,* 1999. Tides for a convective Earth. J. Geophys. Res., **104**, B1, 1035-1058.

5. *Ducarme B., Sun H.-P., Xu J.-Q.*, 2002. New investigation of tidal gravity results from GGP network. Proc. GGP Workshop, Jena, March 11-15,2002. Bull .Inf. Marées Terrestres, **136**, 10761-10776
6. *Groten, E., Molodensky, S.M.*, 1966. Anelastic properties of the mantle and Love numbers consistent with modern VLBI-data. J. of Geodesy, **270**, 1, 603–621.
7. *Karmaleeva R.M.*, 1999. Time variations in tidal wave amplitudes from strain data obtained at the strainmeter station Protvino. Izvestiya, Physics of the Solid Earth, **35**, No 5, 429–433.
8. *Latynina L.A., Boyarsky E.A., Vasil'ev I.M., Sorokin V.L.*, 1997. Tiltmeter measurements at the Protvino station, Moscow region. Izvestiya, Physics of the Solid Earth, **33**, No 11, 949–956.
9. *.Latynina L.A. and Boyarsky E.A.*, 2000. Seasonal Earth tide variations as a model of earthquake precursor. Volcanology and Seismology, **21**, 587–595.
10. *Mathews, P.M., Herring, T.A., Buffett, B.A.*, 2002. Modeling of nutation-precession: New nutation series for nonrigid Earth and insights into the Earth's interior. Journal of Geophysical Research (under press).
11. *Merriam J.B.,* 1994: The nearly diurnal free wobble resonance in gravity measured at Cantley, Quebec // Geophys. J. Int., **119**, 369–380.
12. *Latynina, L.A.,* 1983. Manifestation of the liquid core resonance effects in tide strains. Bull. Inf. Marées Terrestres. **90**, 5938–5951.
13. *Melchior, P.*, 1972. Physique et dynamique planetaires, V. 3 (Geodynamique). Observatoire Royal de Belgique.
14. *Molodensky, M.S.*, 1961. The theory of nutation and diurnal Earth tides // Communs. Obs. R. Belg., 288, 25–56.
15. *Molodensky, S.M.*, 1999. Models of tidal deformations of the Earth consistent with data on its forced nutation // Izvestiya, Physics of the Solid Earth, **35**, 4, 1999, 255–259.
16. *Polzer, G., Zűrn, W., Wenzel H.-G.,* 1996. NDFW analysis of gravity, strain and tilt data from BFO. Bull. Inf. Marees Terrestres. **125**, 9514–9545.
17. *Srarkov V.I., Latyninna L.A., Karmaleeva R.M., Rissaieva S.D., Starkova E.Ya, Mardonov B.*, 1992. Pramètres des déformations de marée à Djerino d'après les résultats de 19 années d'observations. Bull. Inf. Marees Terrestres, **112**, 8177–8186.
18. *Wahr, J.M.*, 1981. Body tides on an elliptical, rotating, elastic and oceanless earth. Geophysical Journal of the Royal astronomical Society, **64**, 677–703.
19. *Wenzel, H.-G.,* 1996. The nanogal software: Earth tide data processing package ETERNA 3.30. Bull. Inf. Marees Terrestres, **124**, 9425–9439.
20. *Yanshin A.L., Melchior, P., Keilis-Borok, V.I., De Brcker, M., Ducarme, B., and Sadovsky A.M.,* 1986. Global distribution of tidal anomalies and an attempt of its geotectonic interpretation. Proc. 10th Int. Symp. On Earth Tides, Madrid. Consejo Sup. Investigaciones Cientificas, Madrid, 731–756.

Table 1.Ratio of amplitude factors of waves P1 and K1 to amplitude factor of wave O1.

Observation interval	Extenso-meter	Total time interval	Number of observation, days	Ratio of amplitude factors		Standard residual, nstr
				φP1 / φO1	φK1 / φO1	
NS component						
1995–1997	NS–1	703	456	0.60±0.04	0.62±0.02	5.2
1997–1999	NS–1	808	391	0.77±0.07	0.30±0.01	3.8
1999–2000	NS–1	619	601	1.01±0.03	0.37±0.01	3.4
Average				0.79	0.43	
Rated value				0.90	0.65	
EW component						

1995–1997	**EW–3**	**707**	**460**	**0.88±0.04**	**0.84±0.02**	**2.6**
1997–1999	**EW–3**	**407**	**481**	**0.96±0.03**	**0.85±0.02**	**3.6**
1999–2000	EW–1	619	577	1.11±0.02	0.76±0.01	4.0
	EW–2	619	*578*	*1.09±0.02*	*0.75±0.01*	*4.1*
	EW–3	619	600	**1.09±0.02**	**0.71±0.01**	**3.9**
Average				1.01*	0.80*	
Rated value				0.94	0.80	

* For calculation of the average value extensometers EW–1 and EW–2 were taken with weight 0.5, as they are two sensors at one common tube.

Table 2. Results of harmonic analysis of observation in 1999–2000.

Extensometer NS–1.

	Wave group	Amplitude measured, nstr	Ratio signal/noise	Amplitude factor and its r.m.s.e.		Phase lead, deg. and its r.m.s.e.	
1	Q1	00629	14.3	0.7882	0.0551	–25.94	3.15
2	O1	2.920	63.6	0.7006	0.0110	–1.67	0.63
3	M1	0.312	4.3	0.9513	0.2213	18.88	12.67
4	P1	1.378	32.6	0.7104	0.0218	124.65	1.25
5	S1	3.088	51.8	67.3428	1.2988	–65.56	74.40
6	K1	1.522	33.4	0.2597	0.0078	39.56	0.45
7	PSI1	0.907	21.3	19.7902	0.9310	–23.88	53.35
8	PHI1	0.591	13.7	7.0819	0.5170	–26.78	29.61
9	J1	0.208	5.1	0.6336	0.1236	20.49	7.08
10	OO1	0.160	2.7	0.8942	0.3358	–12.57	19.24
11	2N2	0.175	5.6	0.5773	0.1028	8.14	5.89
12	N2	1.287	32.4	0.6787	0.0209	3.01	1.20
13	M2	6.755	166.7	0.6818	0.0041	6.60	0.23
14	L2	0.219	5.7	0.7832	0.1373	–8.32	7.87
15	S2	3.319	79.2	0.7200	0.0091	37.92	0.52
16	K2	0.744	15.3	0.5938	0.0387	–21.38	2.22
17	M3	0.039	1.0	0.9519	0.9101	–106.36	52.15

Table 3. Results of harmonic analysis of observation in 1999–2000. Extensometer EW–1.

	Wave group	Amplitude measured, nstr	Ratio signal/noise	Amplitude factor and its r.m.s.e.		Phase lead, deg. and its r.m.s.e.	
1	Q1	0.832	15.7	0.6565	0.0417	–5.69	2.39
2	O1	4.874	90.9	0.7366	0.0081	2.86	0.46
3	M1	0.809	11.4	1.5544	0.1368	–27.85	7.84
4	P1	2.514	51.0	0.8164	0.0160	65.62	0.92
5	S1	2.202	31.7	30.2460	0.9538	–75.40	54.66
6	K1	5.192	97.4	0.5579	0.0057	28.89	0.33
7	PSI1	0.549	11.0	7.5463	0.6838	0.83	39.16
8	PHI1	0.834	16.6	6.2927	0.3795	–39.34	21.74
9	J1	0.538	10.7	1.0348	0.0970	–9.49	5.56
10	OO1	0.394	5.8	1.3853	0.2395	–33.22	13.72
11	2N2	0.064	1.4	4.074	3.0007	–132.62	171.93
12	N2	0.256	4.2	2.6189	0.6203	108.17	35.53
13	M2	0.547	11.5	1.0694	0.0930	5.26	5.32
14	L2	0.110	3.7	4.3821	1.1982	93.79	68.64
15	S2	1.630	33.1	6.8520	0.2070	–99.80	11.85
16	K2	0.266	4.8	4.1143	0.8625	18.09	49.41
17	M3	0.056	1.3	35.6112	27.4674	–30.80	1573.78

Table 4. Results of harmonic analysis of observation in 1999–2000. Extensometer EW–2.

	Wave group	Amplitude measured, nstr	Ratio signal/noise	Amplitude factor and its r.m.s.e.		Phase lead, deg. and its r.m.s.e.	
1	Q1	0.841	16.0	0.6640	0.0415	–6.09	2.33
2	O1	4.920	92.1	0.7436	0.0081	1.95	0.46
3	M1	0.741	10.5	1.4230	0.1358	–36.96	7.04
4	P1	2.507	51.0	0.8142	0.0160	64.32	0.91
5	S1	2.397	34.7	32.9259	0.9500	–73.56	54.46
6	K1	5.176	97.3	0.5562	0.0057	28.23	0.33
7	PSI1	0.602	12.1	8.2650	0.6809	13.33	39.02
8	PHI1	0.812	16.2	6.1258	0.3782	–44.23	21.67
9	J1	0.522	10.4	1.0026	0.0965	–9.00	5.57
10	OO1	0.457	6.7	1.6037	0.2384	–34.28	13.66
11	2N2	0.068	1.5	4.3796	2.9713	–154.20	170.26
12	N2	0.238	3.9	2.4352	0.6166	97.94	35.32
13	M2	0.495	10.5	0.9685	0.0926	5.83	5.49

14	L2	0.081	2.7	3.2416	1.1929	95.56	68.35
15	S2	1.707	34.8	7.1766	0.2064	–99.45	11.41
16	K2	0.260	4.7	4.0196	0.8602	20.14	49.28
17	M3	0.082	1.9	51.8937	27.36890	–25.94	1568.17

Table 5. Results of harmonic analysis of observation in 1999–2000. Extensometer EW–3.

	Wave group	Amplitude measured, nstr	Ratio signal/noise	Amplitude factor and its r.m.s.e.		Phase lead, deg. and its r.m.s.e.	
1	Q1	0.769	14.9	0.6067	0.0407	–6.37	2.08
2	O1	5.108	96.5	0.7720	0.0080	1.55	0.46
3	M1	0.727	10.2	1.3970	0.1368	–30.59	7.93
4	P1	2.582	52.7	0.8386	0.0159	63.29	0.91
5	S1	2.303	33.3	31.6374	0.9514	–78.68	54.53
6	K1	5.242	99.0	0.5633	0.0057	25.07	0.33
7	PSI1	0.560	11.3	7.6904	0.6819	-4.44	39.07
8	PHI1	0.721	14.4	5.4414	0.3767	–48.06	21.58
9	J1	0.473	9.6	0.9086	0.0948	–0.45	5.26
10	OO1	0.440	6.4	1.5467	0.2417	–30.90	13.85
11	2N2	0.115	2.5	7.3522	2.9357	-129.32	168.21
12	N2	0.207	3.5	2.1146	0.6097	104.08	34.93
13	M2	0.368	7.8	0.7202	0.0921	–33.30	5.51
14	L2	0.076	2.6	3.0328	1.1753	110.88	67.35
15	S2	1.840	37.9	7.7354	0.2043	-98.77	11.70
16	K2	0.251	4.6	3.8798	0.8495	21.98	48.67
17	M3	0.088	2.1	56.0900	27.2240	–25.62	1559.83

Table 6. Tidal parameters from three parallel extensometer at Protvino.

Wave group	Amplitude, nstr			Phase lead, degree		
	EW–1	EW–2	EW–3	EW–1	EW–2	EW–3
Q1	0.832	0.841	0.769	–5.69	–6.09	–6.37
O1	4.874	4.920	5.108	2.86	1.95	1.55
M1	0.809	0.741	0.727	–27.85	–36.96	–30.59
P1	2.514	2.507	2.582	65.62	64.32	63.29
S1	2.202	2.397	2.303	–75.40	–73.56	–78.68
K1	5.192	5.176	5.242	28.89	28.23	25.07
PSI1	0.549	0.602	0.560	0.83	13.33	-4.44
PHI1	0.834	0.812	0.721	–39.34	–44.23	–48.06
J1	0.538	0.522	0.473	–9.49	–9.00	–0.45
OO1	0.394	0.457	0.440	–33.22	–34.28	–30.90
2N2	0.064	0.068	0.115	–132.62	–154.20	-129.32
N2	0.256	0.238	0.207	108.17	97.94	104.08
M2	0.547	0.495	0.368	5.26	5.83	–33.30
L2	0.110	0.081	0.076	93.79	95.56	110.88
S2	1.630	1.707	1.840	–99.80	–99.45	-98.77
K2	0.266	0.260	0.251	18.09	20.14	21.98
M3	0.056	0.082	0.088	–30.80	–25.94	–25.62

Table 7. Results of harmonic analysis of observation in 1999–2000 with compensation of temperature and atmospheric pressure variations.

Compo-nent, exten-someter	Amplitude, nstr		Ratio of amplitude factors		Standard residual, nstr	Response	
	O1	S1	φP1 / φO1	φK1 / φO1		Temperat.	Pressure
No weather effects accounted							
NS–1	2.920	3.088	1.014 ±0.035	0.371 ±0.012	3.444	—	—
EW–1	4.874	2.202	1.108 ±0.025	0.757 ±0.011	3.958	—	—
EW–2	*4.920*	*2.397*	*1.095 ±0.024*	*0.748 ±0.011*	*3.944*	—	—
EW3	**5.108**	**2.303**	**1.086 ±0.024**	**0709 ±0.010**	**3.973**	—	—
With response to outer temperature							
NS–1	2.913	0.990	0.404 ±0.030	0.528 ±0.135	3.176	–0.941	—
EW–1	4.875	0.695	1.101 ±0.024	0.823 ±0.012	3.833	–0.688	—
EW–2	*4.926*	*0.554*	*1.103 ±0.024*	*0.813 ±0.012*	*3.757*	*–0.706*	—
EW–3	**5.103**	**0.943**	**1.106 ±0.023**	**0.803 ±0.011**	**3.813**	**–0.782**	—
With response to atmospheric pressure							
NS–1	3.004	2.932	0.930 ±0.030	0.345 ±0.012	3.390	—	0.890
EW–1	4.935	2.054	1.044 ±0.024	0.740 ±0.011	3.929	—	0.699
EW–2	*4.985*	*2.249*	*1.029 ±0.024*	*0.729 ±0.011*	*3.912*	—	*0.737*
EW–3	**5.190**	**2.130**	**1.012 ±0.023**	**0.709 ±0.010**	**3.928**	—	**0.872**
With response to outer temperature and atmospheric pressure							
NS–1	2.958	0.817	0.367 ±0.030	0.502 ±0.013	3.159	–0.890	0.485
EW–1	4.899	0.582	1.067 ±0.024	0.810 ±0.011	3.832	-0.644	0.386
EW–2	*5.121*	*0.461*	*1.065 ±0.024*	*0.799 ±0.012*	*3.938*	*-0.680*	*0.442*
EW–3	**5.175**	**0.774**	**1.054 ±0.022**	**0.780 ±0.011**	**3.800**	**–0.720**	**0.530**
NS	Rated value		0.90	0.65			
EW			0.94	0.80			

Table 8. Elimination of outer temperature effect from measured deformation waves P_1 and K_1 for component NS, 1999–2000

(assuming that temperature affects these waves the same way as S_1)

		P1		S1		K1	
		A	κ	A	κ	A	κ
1	Theoretical value	1.939	0.0	0.046	0.0	5.862	0.0
2	Measured **deformation**, nstr (tide + temperature effect)	1.378	124.6	3.088	–65.6	1.522	39.6
3	Measured **temperature**, C°	1.088	–35.1	4.104	107.2	1.190	–31.7
4	The same A_T and κ_T after the subtracting 180° from phases	–1.088	144.9	–4.104	–72.8	–1.190	148.3
5	Response for S1: [row 2] / [row 4] and shift of phase: [2] minus [4]			–0.7524	7.2		
6	Estimated deformation induced by temperature: $A = –0.7524\ A_T$; $\kappa = \kappa_T + 7.2$	0.819	152.2	3.088	–65.6	0.895	155.6
7	Deformation without temperature effect: [2] minus [6]	0.755	94.5	0.000	—	2.077	16.8
8	Amplitude factor: [7] / [0]	0.389				0.354	
9	Amplitude factor divided by that for wave O1: [8] / 0.701	0.556				0.506	
10	Rated value for εP1 and εK1	0.90				0.65	

Table 9. Comparison of the different methods of temperature correction (NS component)

Method (criteria)		τ	R	$s0$	A_{S1}	εP1	εK1	K_{K1}
		(hour)	(nstr/K)	(nstr)	(nstr)			(°)
Without account of temperature		—	—	3.444	3.088	0.404	0.528	39.6
With Account of the integral temperature effect		–2.0	–0.721	3.288	1.200	0.785	0.546	24.9
	Maximum ε_{K1}	–1.0	–0.856	3.223	0.615	0.604	0.550	17.5
	Minimum A_{S1}	–0.8	–0.879	3.210	0.601	0.565	0.547	16.0
		0.0	–0.941	3.176	0.890	0.404	0.528	10.2
	Maximum R, minimum s_0	0.6	–0.956	3.168	1.472	0.327	0.501	6.7
		1.0	–0.951	3.171	1.569	0.266	0.478	4.3
	Minimum k_{K1}	2.0	–0.873	3.215	2.183	0.345	0.407	1.9
		3.0	–0.714		3.293	0.548	0.336	5.9
Temperature and its derivative		0.56	-0.973	3.162	1.318	0.299	0.506	6.2
Elimination of S1 (see Table 8)		–0.48	–0.752	—	0.000	0.566	0.506	16.8

Note: The values for $\tau = –0.8$ and $\tau = 0.6$ are taken from approximations by parabolas based on nearest 4–5 values derived from Eterna program (Fig. 5).

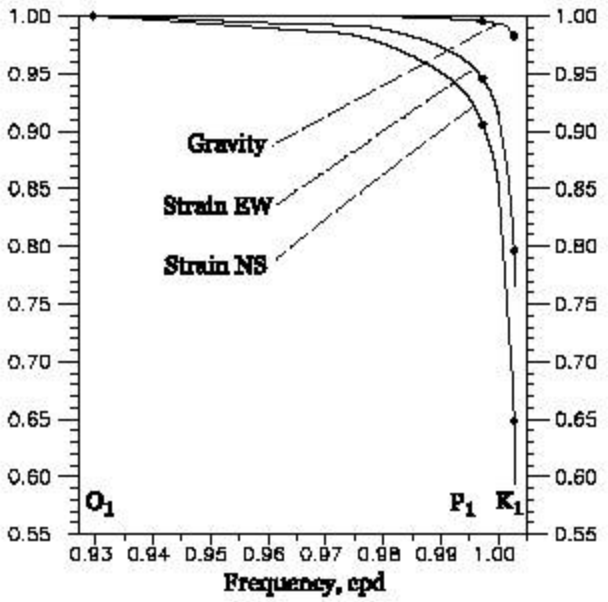

Fig. 1. Relative diminution of tide wave amplitude owing to the liquid core resonanse, according to Wahr [1981].

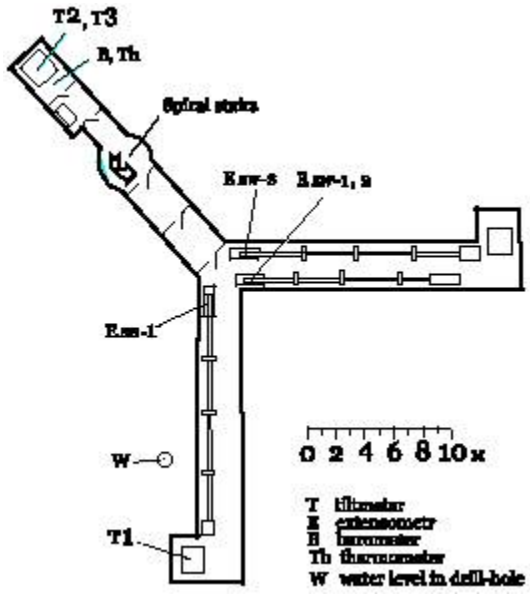

Fig. 2 : Sketch of the Protvino underground station.

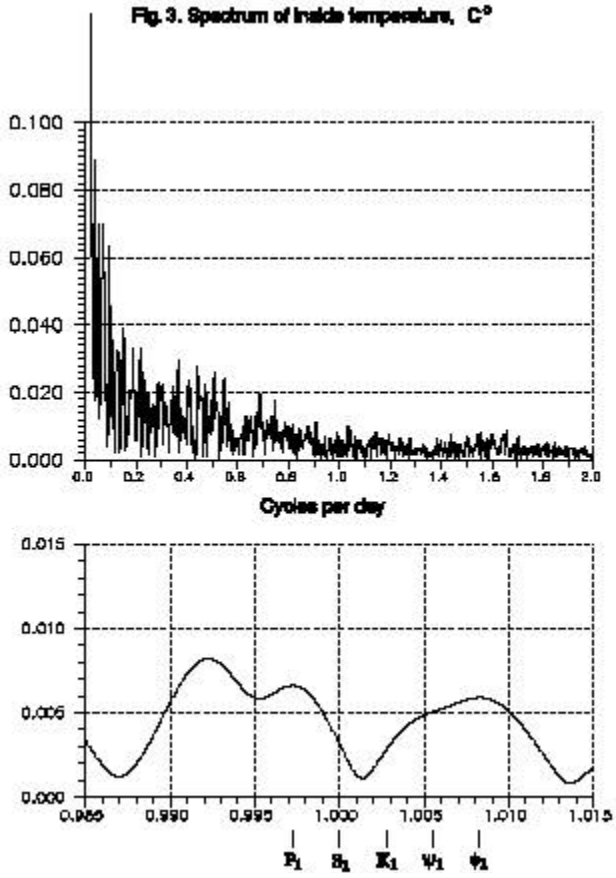

Fig.4. Spectrum of temperature at weather station Serpukhov for three years 1998-2000

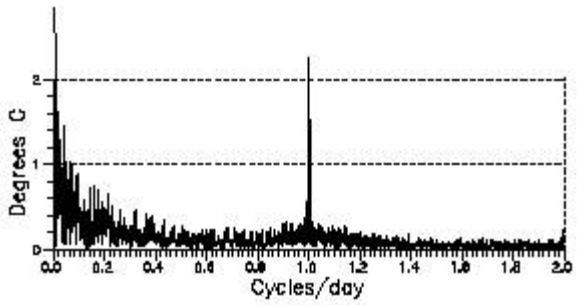

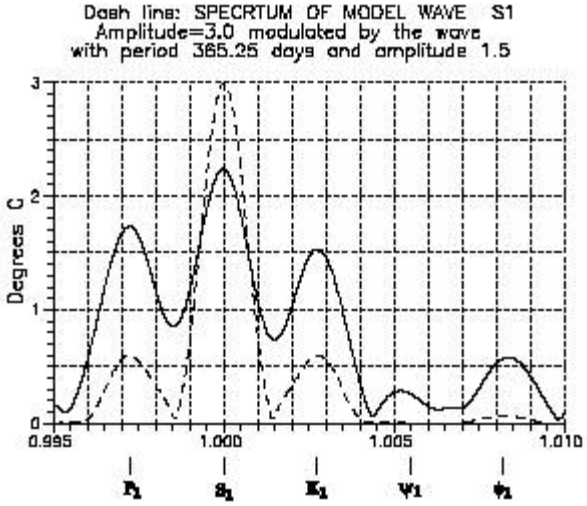

Fig.

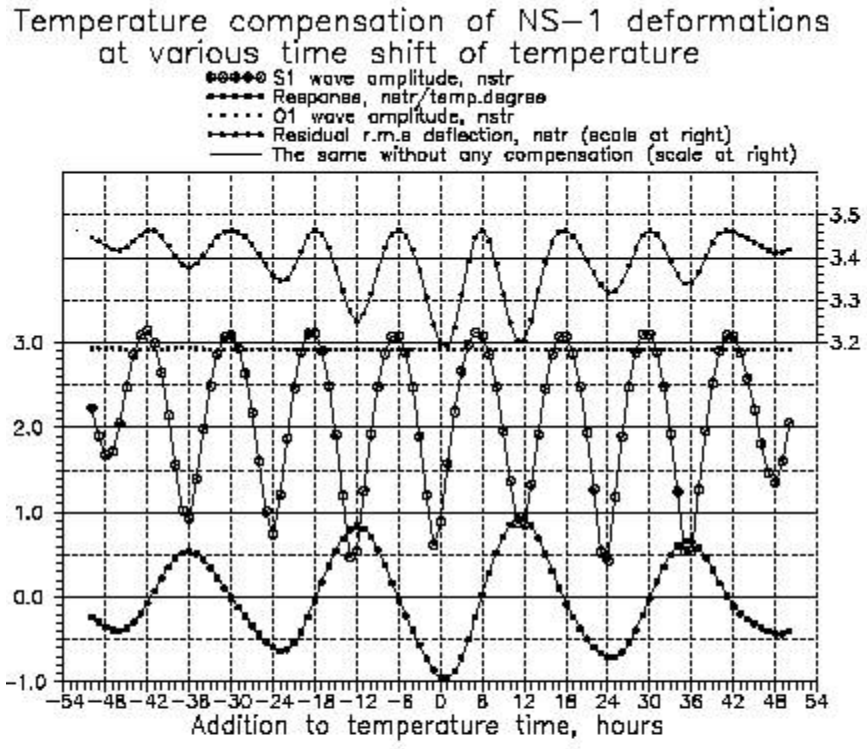
Temperature compensation of NS–1 deformations
at various time shift of temperature
S1 wave amplitude, nstr
Response, nstr/temp.degree
O1 wave amplitude, nstr
Residual r.m.s deflection, nstr (scale at right)
The same without any compensation (scale at right)
3.5
3.4
3.3
3.2
3.0
2.0
1.0
0.0
-1.0
-54 -48 -42 -36 -30 -24 -18 -12 -6 0 6 12 18 24 30 36 42 48 54
Addition to temperature time, hours

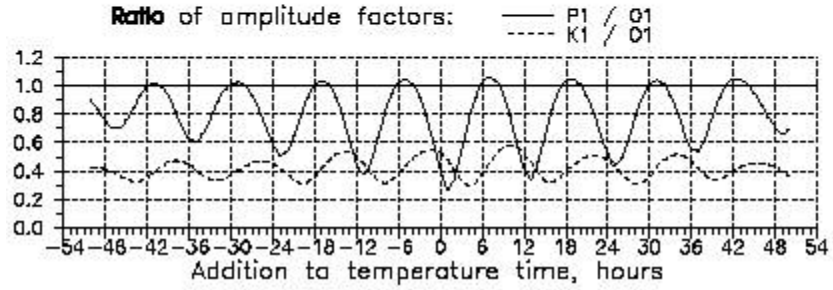
Ratio of amplitude factors:
P1 / O1
K1 / O1
1.2
1.0
0.8
0.6
0.4
0.2
0.0
-54 -48 -42 -36 -30 -24 -18 -12 -6 0 6 12 18 24 30 36 42 48 54
Addition to temperature time, hours

Fig.

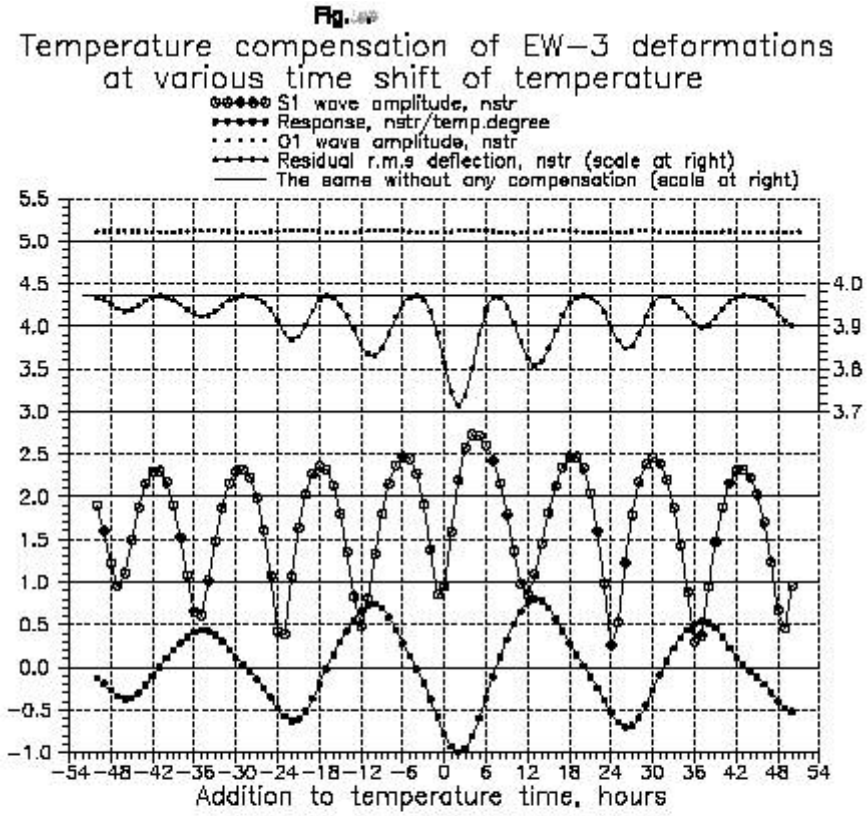
Temperature compensation of EW–3 deformations
at various time shift of temperature
S1 wave amplitude, nstr
Response, nstr/temp.degree
O1 wave amplitude, nstr
Residual r.m.s deflection, nstr (scale at right)
The same without any compensation (scale at right)
5.5
5.0
4.5
4.0
3.5
3.0
2.5
2.0
1.5
1.0
0.5
0.0
−0.5
−1.0
4.0
3.9
3.8
3.7
−54 −48 −42 −36 −30 −24 −18 −12 −6 0 6 12 18 24 30 36 42 48 54
Addition to temperature time, hours

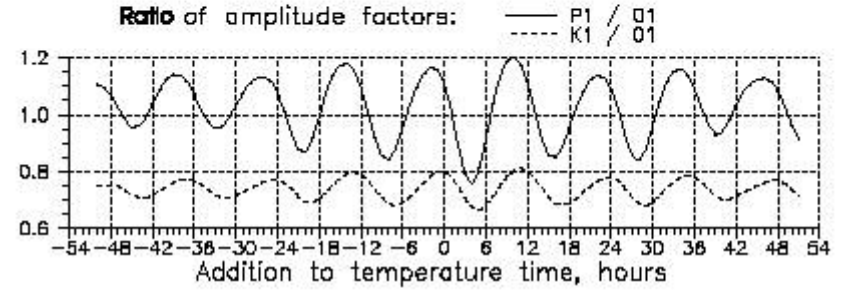
Ratio of amplitude factors:
P1 / O1
K1 / O1
1.2
1.0
0.8
0.6
−54 −48 −42 −36 −30 −24 −18 −12 −6 0 6 12 18 24 30 36 42 48 54
Addition to temperature time, hours

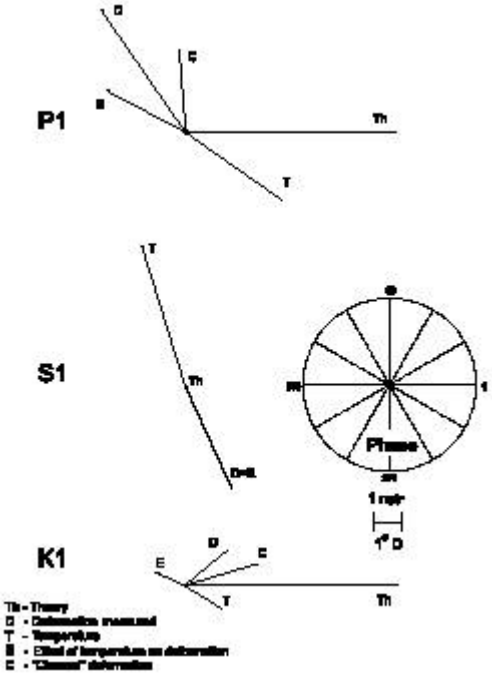
P1
S1
K1
Phase
1 mkr
1° D

Fig. 7 : Vectorial diagram illustrating the correction method based on the elimination of S_1.